Dalton Transactions

PAPER

Anion-directed supramolecular chemistry modulating the magnetic properties of nanoscopic Mn coordination clusters: from polynuclear high-spin complexes to SMMs†

Cite this: DOI: 10.1039/c6dt02642g

Lei Zhang,[a,b] Theresa Chimamkpam,[b] Camelia I. Onet,[b] Nianyong Zhu,[b,c] Rodolphe Clérac[d,e] and Wolfgang Schmitt*[b]

We report a supramolecular approach to mixed-valent Mn coordination clusters that demonstrates how halide ions can be applied to influence the assembly of distinct tetranuclear building units to produce a number of related Mn coordination clusters with dense core structures that derive from a cuboctahedral arrangement of Mn ions. In all compounds the alignment of the Jahn–Teller axes of the Mn^{III} centers coincides with the positions of the stabilizing chloride ligands. Thus, the relative chloride concentrations in the reaction mixtures allow us to modify the symmetry and magnetic anisotropy of this basic core structures resulting in isotropic polynuclear high-spin complexes at high Cl^- concentrations and Single-Molecule Magnets at lower relative Cl^- concentrations.

DOI: 10.1039/c6dt02642g

www.rsc.org/dalton

Introduction

Polynuclear high-spin complexes and single molecule magnets (SMMs) provide highly interesting classes of complexes that can be characterized by magnetocaloric effects or slow relaxation of the magnetization respectively.[1,2] These physicochemical attributes not only promote theoretical studies to understand the origin of these phenomena but moreover can lead to the development of future applications, for instance in cryogenic cooling systems, data storage devices or quantum computers.[3,4] However, the synthesis of larger polynuclear compounds usually involves complex self-assembly processes often resulting in serendipitous products in which building units are randomly organized.[5] Their ground spin states and magnetic anisotropies can in most cases not be controlled.[6] Manganese coordination clusters are probably the most studied systems in this field of research.[7,8] Geometrical arrangements in Mn complexes can give rise to ferromagnetic or uncompensated anti-ferromagnetic interactions between spin centers that may adopt different oxidation states with variable numbers of unpaired electrons. In Mn^{III}-based complexes, the local easy-axis orientation of the single-ion anisotropy tensor is remarkably easy to localize as it coincides with the orientation of the Mn^{III} Jahn–Teller axes. As a consequence, the overall easy-axis of the magnetic anisotropy for polynuclear Mn^{III} species can be determined from the tensorial addition of the local anisotropy tensors respecting the symmetry of the cluster core.[9] Considering these aspects, synthetic concepts or supramolecular approaches that direct the alignment of these Jahn–Teller axes within Mn^{III} coordination clusters should allow one to have at least a partial control of their magnetic properties. It is well established that anions can act as templates or structure-directing agents for the synthesis of metallo-supramolecular complexes and may provide a synthetic means to modify the symmetry and the magnetic properties of complex coordination clusters.[10]

In order to devise a supramolecular concept that aims to organize oligonuclear subunits into defined cluster topologies, one needs to apply a powerful analytical tool to monitor the formation of new species and their aggregation processes in solution or reaction mixtures. Recently, mass spectrometry has been applied effectively for solution characterizations of highly labile and complex coordination and organometallic compounds.[11] Cronin and co-workers demonstrated that mass spectrometry can be used as an exceptionally versatile tool to

[a]State Key Laboratory of Structural Chemistry, Fujian Institute of Research on the Structure of Matter, Chinese Academy of Sciences, Fuzhou, Fujian 350002, P. R. China
[b]School of Chemistry & CRANN, University of Dublin, Trinity College, Dublin 2, Ireland. E-mail: schmittw@tcd.ie; Fax: +353-1-6712826; Tel: +353-1-8963495
[c]Institute of Molecular Functional Materials & Department of Chemistry, Hong Kong Baptist University, Waterloo Road, Hong Kong, China
[d]CNRS, CRPP, UPR 8641, Pessac F-33600, France
[e]Univ. Bordeaux, CRPP, UPR 8641, F-33600 Pessac, France

†Electronic supplementary information (ESI) available: Full experimental procedures and crystallographic data in CIF format for the new structures. CCDC 1062487–1062490. For ESI and crystallographic data in CIF or other electronic format see DOI: 10.1039/c6dt02642g

monitor the self-assembly of polyoxometalates or identify new POM clusters that emerge in solution.[12] Surprisingly, similar mass-spectrometric approaches have not been applied for the investigation of Mn coordination clusters although these often show structural characteristics that are comparable to polyoxometalates.

Previously we demonstrated that com-proportion reactions can be applied to selectively prepare Mn^{III} clusters and we highlighted that the kinetic liability of the Jahn–Teller sites allows their selective functionalisation.[13] Here we report a supramolecular approach using halides to influence the arrangement of the Jahn–Teller distorted Mn^{III} centres. This underlying methodology now allows us to systematically modify the topologies and the magnetic properties of a homologue series of complex Mn coordination clusters. In all here reported compounds the alignment of the Jahn–Teller axes coincides with the positions of the stabilizing halide ligands (Cl^-). This kind of synthetic strategy to systematically modulate the structures of highly complex, high-nuclearity compounds has never been applied so far.

In the presence of high halide concentrations we obtain a tridecanuclear Keplerate **$Mn_{13}P_8 \subset Cl_6$** with cuboctahedral Keggin-type arrangement of the Mn^{III} centres in which 6 chloride anions adopt an octahedral topology with each ion capping a square face of the polygon.[13a] Upon lowering the halide concentrations the cluster core is basically maintained and **$Mn_{12}P_{10} \subset Cl_4$**, **$Mn_{13}P_{10} \subset Cl_4$**, **$Mn_{14}P_{11} \subset Cl_4$** and **$Mn_{15}P_{10} \subset Cl_4$** are obtained (Table 1). In these polynuclear complexes, only four halide ions stabilize four square cluster faces and one vertex of the cuboctahedron has been displaced to give lacunary Keggin-type derivatives. In this class of compound the Mn^{III} centres are ferromagnetically coupled leading to high-spin ground states whilst the maintained symmetry gives rise to a negligible magnetic anisotropy. When the structure-directing influence of the halide ions is further suppressed the former cuboctahedral arrangement undergoes distortion, fewer square faces are capped by the halide ions and a compound with lower symmetry is obtained, **$Mn_{15}P_{12} \subset Cl_2$**. This compound is characterized by competing anti- and ferromagnetic interactions and an increased magnetic anisotropy giving rise to Single-Molecule Magnet (SMM) properties. In addition, we prove that mass spectrometry can be a highly efficient tool to monitor complex condensation reactions allowing us to identify new Mn cluster species that are stable in solution.

Results and discussion

The archetype structure

The com-proportionation reaction using $KMnO_4$ and $MnCl_2{\cdot}4H_2O$ in acetonitrile in the presence of *tert*-butyl-PO_3H_2 results in mixed-valent, high-nucleartiy complexes with high Mn^{III} content. The archetype structure that can be obtained at Cl : *tert*-butyl-PO_3H_2 ratio of 6 : 1 is a highly symmetric Mn-based Keplerate, $[Mn^{II}Mn^{III}_{12}(\mu_4\text{-}O)_8(\mu_4\text{-}Cl)_6(\textit{tert}\text{-butyl-}PO_3)_8]$ (**$Mn_{13}P_8 \subset Cl_6$**), in which the Mn^{III} ions form a cuboctahedral arrangement and the Cl^- ions cap the six square faces to adopt an octahedral $\{Cl_6\}$ topology (Fig. 1). The core of this

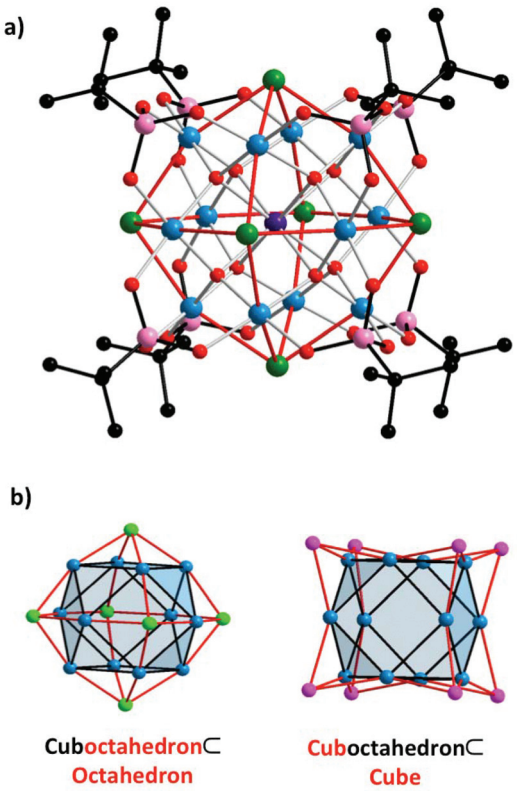

Fig. 1 (a) Crystal structure of the archetype $[Mn^{II}Mn^{III}_{12}(\mu_4\text{-}O)_8(\mu_4\text{-}Cl)_6(\textit{tert}\text{-butyl-}PO_3)_8]$ cluster (**$Mn_{13}P_8 \subset Cl_6$**).[13a] (b) Representation of the cuboctahedral arrangement of Mn^{III} centres whereby the stabilizing Cl^- ions cap the 6 rectangular faces (left) and the P atoms of the phosphonate ligands cap the 8 triangular faces (right). Color code: Mn^{II} violet, Mn^{III} light blue, P pink, Cl green, O red, C black.

Table 1 Overall composition of the novel compounds that crystallise under the reported conditions and contain the discussed coordination clusters

Abbreviation	Overall composition of the reported compounds that that crystallise under the reported conditions and contain the coordination clusters
$Mn_{12}P_{10} \subset Cl_4$	$A_2[Mn^{II}_3Mn^{III}_9(\mu_4\text{-}O)_6(\mu_3\text{-}OH)_2(\mu_4\text{-}Cl)_4(\textit{tert}\text{-butyl-}PO_3H)_3(\textit{tert}\text{-butyl-}PO_3)_7]{\cdot}2.5H_2O{\cdot}6CH_3CN$ (**I**), A = $[Mn^{III}_6(\textit{tert}\text{-butyl-}PO_3)_8(\text{pyridine})_6(Cl)]$
$Mn_{13}P_{10} \subset Cl_4$	$A[Mn^{II}_2Mn^{III}_{11}(\mu_4\text{-}O)_6(\mu_3\text{-}O)(\mu_3\text{-}OH)(\mu_4\text{-}Cl)_4(\textit{tert}\text{-butyl-}PO_3H)(\textit{tert}\text{-butyl-}PO_3)_9(H_2O)]{\cdot}2H_2O{\cdot}9CH_3CN$ (**II**), A = $[Mn^{III}_6(\textit{tert}\text{-butyl-}PO_3)_8(\text{pyridine})_6(Cl)]$
$Mn_{15}P_{10} \subset Cl_4$	$A[Mn^{II}_3Mn^{III}_{12}(\mu_4\text{-}O)_6(\mu_3\text{-}O)_2(\mu_3\text{-}OH)(\mu_4\text{-}Cl)_4(Cl)_2(\textit{tert}\text{-butyl-}PO_3)_{10}(H_2O)(\text{pyridine})_2]{\cdot}2H_2O{\cdot}CH_3CN$ (**III**), A = $[Mn^{III}_6(\textit{tert}\text{-butyl-}PO_3)_8(\text{pyridine})_6(Cl)]$
$Mn_{15}P_{12} \subset Cl_2$	$(2\text{-amino-Hpyridine})_2[Mn^{II}_3Mn^{III}_{12}(\mu_4\text{-}O)_8(\mu_4\text{-}Cl)_2(\mu_2\text{-}CH_3O)_4(CH_3OH)_2(\textit{tert}\text{-butyl-}PO_3H)_2(\textit{tert}\text{-butyl-}PO_3)_{10}]{\cdot}8H_2O{\cdot}3CH_3OH$ (**IV**)

polynuclear complex contains a central Mn^{II} ion that links *via* 8 μ_4-O^{2-} ligands to the surrounding Mn^{III} atoms. A remarkable feature of **$Mn_{13}P_8 \subset Cl_6$** is its solution-stability in polar solvents resulting in mass spectra with a clearly distinctive signal centered at *m*/*z* 1079.0. This cluster motif is closely related to the recently discovered Pd-based polyoxometalates,[14] highlighting the close structural relationship between these Mn coordination clusters and polyoxometalates. Indeed, the **$Mn_{13}P_8 \subset Cl_6$** Keplerate-structure reveals attributes that are comparable to our previously investigated polyoxovanadate system in which halides template the assembly of homologous clusters cores.[10a]

MALDI-MS approach to characterize new structurally-related species

To investigate a potential structure-directing influence of Cl^- ions on the formation of this class of Mn coordination cluster, different synthetic conditions involving variable Cl : *tert*-butyl-PO_3H_2 ratios were investigated. The resulting reaction mixtures were screened by MS analyses to identify potentially related new species (Fig. 2d). Whilst electrospray (ESI) and cryospray mass spectrometry (CSI-MS) techniques are widely applied for analyses of POM clusters, we found that matrix-assisted laser desorption/ionization mass spectrometry (MALDI-MS) was more suitable to characterize the solution behavior of the high-nuclearity Mn systems as this method resulted in signals of mono-charged species in the high-mass regions rather than in overlapping signals of fragments in the lower mass region.[15] The investigation of a reaction mixture containing a Cl : *tert*-butyl-PO_3H_2 mole ratio of 3 : 1 and pyridine co-ligands, proved to be most informative. The resulting negative-mode spectrum does not contain typical signals arising from the former **$Mn_{13}P_8 \subset Cl_6$** species but is characterized by a series of new signals in the range of *m*/*z* 2100 and 2600, indicative for the formation of new high-nuclearity Mn complexes. The detailed assignment of the signals of this rather complex reaction mixture was aided by single crystal X-ray analyses of three different cluster species **$Mn_{12}P_{10} \subset Cl_4$**, **$Mn_{13}P_{10} \subset Cl_4$** and **$Mn_{15}P_{10} \subset Cl_4$** that co-crystallized from this reaction mixture (Fig. 2). All these polynuclear complexes are negatively charged and whereby the recently reported 'Chevrel-type' coordination cluster $[Cl \subset Mn_6(tert\text{-butyl-}PO_3)_8]^+$ facilitates the charge balance in these inter-clusters compounds (see ESI, Fig. S7†).[13c]

The MS assignment provided a fingerprint spectrum of characteristic signals which in consecutive analyses allowed us

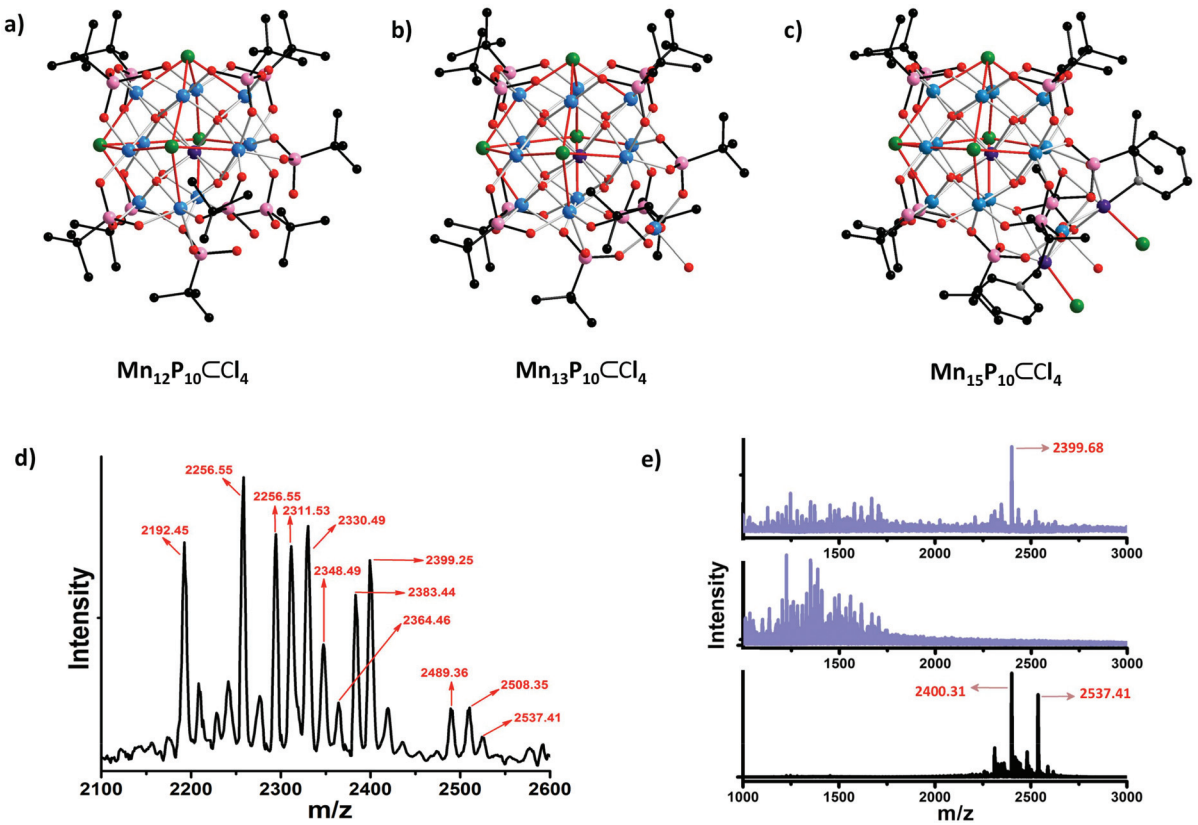

Fig. 2 (a)–(c) Crystal structures of (a) **$Mn_{12}P_{10} \subset Cl_4$** in **I**, (b) **$Mn_{13}P_{10} \subset Cl_4$** in **II**, and (c) **$Mn_{15}P_{10} \subset Cl_4$** in **III**. Color code: Mn^{II} violet, Mn^{III} light blue, P pink, Cl green, O red, C black, N grey. (d) Negative-mode MALDI-MS spectra to monitor the co-crystallization of **$Mn_{12}P_{10} \subset Cl_4$**, **$Mn_{13}P_{10} \subset Cl_4$**, **$Mn_{15}P_{10} \subset Cl_4$**: reaction mixture 24 h after preparation. Signal assignment is provided in Table 2. (e) Negative-mode MALDI-MS spectra to identify the **$Mn_{15}P_{10} \subset Cl_4$** cluster: (upper) reaction mixture 24 h after preparation; (middle) reaction mixture after crystallization of **$Mn_{15}P_{10} \subset Cl_4$**; (bottom) crystals of **$Mn_{15}P_{10} \subset Cl_4$** re-dissolved in CH_3CN.

Table 2 MS-analysis of the reaction system: characteristic species that originate from $\mathbf{Mn_{12}P_{10} \subset Cl_4}$, $\mathbf{Mn_{13}P_{10} \subset Cl_4}$, and $\mathbf{Mn_{15}P_{10} \subset Cl_4}$ and that can be detected in reaction mixtures using negative mode MALDI-MS experiments

Species	Calculated *m*/*z*	Experimental *m*/*z*
$[Mn_{12}(\mu_4\text{-}O)_6(\mu_3\text{-}OH)_2(\textit{tert}\text{-butyl-}PO_3H)_2(\textit{tert}\text{-butyl-}PO_3)_8(CH_3CN)]^-$	2192.56	2192.45
$[Mn_{13}(\mu_4\text{-}O)_6(\mu_3\text{-}O)(\mu_3\text{-}OH)(\mu_4\text{-}Cl)(\textit{tert}\text{-butyl-}PO_3)_{10}(H_2O)]^-$	2256.43	2256.55
$[Mn_{13}(\mu_4\text{-}O)_6(\mu_3\text{-}O)(\mu_3\text{-}OH)(\mu_4\text{-}Cl)_2(\textit{tert}\text{-butyl-}PO_3H)(\textit{tert}\text{-butyl-}PO_3)_9(H_2O)]^-$	2292.41	2292.52
$[Mn_{13}(\mu_4\text{-}O)_6(\mu_3\text{-}O)(\mu_3\text{-}OH)(\mu_4\text{-}Cl)_3(\textit{tert}\text{-butyl-}PO_3H)(\textit{tert}\text{-butyl-}PO_3)_9]^-$	2311.36	2311.53
$[Mn_{13}(\mu_4\text{-}O)_6(\mu_3\text{-}O)(\mu_3\text{-}OH)(\mu_4\text{-}Cl)_3(\textit{tert}\text{-butyl-}PO_3H)_2(\textit{tert}\text{-butyl-}PO_3)_8(H_2O)]^-$	2330.38	2330.49
$[Mn_{13}(\mu_4\text{-}O)_6(\mu_3\text{-}OH)_2(\mu_4\text{-}Cl)_4(\textit{tert}\text{-butyl-}PO_3H)_2(\textit{tert}\text{-butyl-}PO_3)_8]^-$	2348.35	2348.49
$[Mn_{13}(\mu_4\text{-}O)_6(\mu_3\text{-}O)(\mu_3\text{-}OH)(\mu_4\text{-}Cl)_4(\textit{tert}\text{-butyl-}PO_3H)(\textit{tert}\text{-butyl-}PO_3)_9(H_2O)]^-$	2364.34	2364.46
$[Mn_{13}(\mu_4\text{-}O)_6(\mu_3\text{-}O)(\mu_3\text{-}OH)(\mu_4\text{-}Cl)_4(\textit{tert}\text{-butyl-}PO_3H)_2(\textit{tert}\text{-butyl-}PO_3)_8(H_2O)_2]^-$	2383.36	2383.44
$[Mn_{15}(\mu_4\text{-}O)_6(\mu_3\text{-}O)_2(\mu_3\text{-}OH)(\mu_4\text{-}Cl)_2(\textit{tert}\text{-butyl-}PO_3)_{10}]^-$	2399.26	2399.25
$[Mn_{15}(\mu_4\text{-}O)_6(\mu_3\text{-}O)_2(\mu_3\text{-}OH)(\mu_4\text{-}Cl)_4(\textit{tert}\text{-butyl-}PO_3)_{10}(H_2O)]^-$	2489.21	2489.36
$[Mn_{15}(\mu_4\text{-}O)_6(\mu_3\text{-}O)(\mu_3\text{-}OH)_2(\mu_4\text{-}Cl)_4(\textit{tert}\text{-butyl-}PO_3)_{10}(H_2O)_2]^-$	2508.22	2508.35
$[Mn_{15}(\mu_4\text{-}O)_6(\mu_3\text{-}O)_2(\mu_3\text{-}OH)(\mu_4\text{-}Cl)_4(\textit{tert}\text{-butyl-}PO_3)_{10}(O)_2(OH)_2]^-$	2537.19	2537.41

to identify key species in solution, optimize their formation conditions to prepare phase-pure samples of $\mathbf{Mn_{13}P_{10} \subset Cl_4}$, $\mathbf{Mn_{14}P_{11} \subset Cl_4}$ and $\mathbf{Mn_{15}P_{10} \subset Cl_4}$ at slightly variable reaction conditions; although the identity of $\mathbf{Mn_{12}P_{10} \subset Cl_4}$ was clearly established by single-crystal X-ray diffraction and MS-analyses, this compound could not be obtained in a phase-pure form (Fig. 2, Tables 1 and 2). The other polynuclear species could clearly be identified in solution using MS spectrometry. The assignment of the signals is provided in Fig. 2d and Table 2. The successful simulation of the isotopic envelopes of the most characteristic species further confirms their identity and solution stability (see ESI†).

Key-features of the reaction system and of the assembly of the polynuclear complexes

From the structural analyses one can conclude that the assembly of these Mn coordination clusters is governed by *tert*-butylphosphonates that preferentially adopt a cubic arrangement whereby each phosphonate group ideally acts a $\eta^1{:}\eta^1{:}\eta^1{:}\mu_3$ bridging ligand (Fig. 2). The binding mode results in square arrangements of four metal centers that rely on the stabilization by μ_4-Cl^- ligands. When the Cl : *tert*-butyl-PO_3H_2 ratio is reduced, not all the square faces can be stabilized by Cl^- ions; the square arrangement of some Mn centers can not be retained. Thus in comparison to the archetype $\mathbf{Mn_{13}P_8 \subset Cl_6}$ complex, in $\mathbf{Mn_{12}P_{10} \subset Cl_4}$ two former positions of the capping Cl^- ions are replaced by two *tert*-butyl-phosphonate ligands, resulting in the removal of one vertex of the cuboctahedron. All remaining square faces of the resulting lacunary-cuboctahedron are capped by Cl^- anions. The structure of $\mathbf{Mn_{12}P_{10} \subset Cl_4}$ may be regarded as an intermediate species towards the assembly of $\mathbf{Mn_{13}P_{10} \subset Cl_4}$ and $\mathbf{Mn_{15}P_{10} \subset Cl_4}$ which results from the formal attachment of an additional Mn^{III} center or a triangular $\{(\mu_3\text{-}OH)Mn^{II}_2Mn^{III}\}$ subunit to the $\{Mn^{II}Mn^{III}_{11}\}$ core structure, respectively. In $\mathbf{Mn_{14}P_{11} \subset Cl_4}$, a dinuclear {Mn–OH–Mn} unit is attached to the $\{Mn^{II}Mn^{III}_{11}\}$ core involving an additional phosphonate ligand. It is important to state that in all structures, Cl^- ligands locate at the Jahn–Teller sites of the tetragonally elongated Mn^{III} coordination environments (Fig. 3a).

Table 3 summarizes the structures and the Cl : *tert*-butyl-PO_3H_2 ratios clearly highlighting the characteristics of the halide-influenced supramolecular assembly process. At a Cl : P mole ratio of 6 : 1, six Cl^- ions stabilize the cuboctahedral assembly of six corner-sharing $\{Mn_4\}$ squares in $\mathbf{Mn_{13}P_8 \subset Cl_6}$. Two *tert*-butylphosphonate ligands formally replace two Cl^- when the Cl : P mole ratio is lowered to 4 : 1 or 3 : 1, resulting in the described lacunary-cuboctahedra in $\mathbf{Mn_{12}P_{10} \subset Cl_4}$, $\mathbf{Mn_{13}P_{10} \subset Cl_4}$ and $\mathbf{Mn_{15}P_{10} \subset Cl_4}$. Higher *tert*-butylphosphonate concentrations at a Cl : P mole ratio of 2 : 1, promote the formation of $\mathbf{Mn_{14}P_{11} \subset Cl_4}$ which contains an additional phosphonate ligand.

Ferromagnetic intra-cluster interactions to give high spin ground states

Studies of the magnetic properties of $\mathbf{Mn_{13}P_8 \subset Cl_6}$, $\mathbf{Mn_{13}P_{10} \subset Cl_4}$, and $\mathbf{Mn_{14}P_{11} \subset Cl_4}$ were conducted on powdered samples (Fig. 3b and d). These demonstrate that the cuboctahedral arrangement of Mn^{III} centers around a central Mn^{II} metal ion gives rises to significant ferromagnetic interactions between the Mn spin centers to stabilize a high-spin ground states of $S \geq 35/2$,[13a] in agreement with the χT data and the field-dependence of the magnetization, M. Similar studies on $\mathbf{Mn_{15}P_{10} \subset Cl_4}$ reveal a room temperature χT product of 77.5 cm^3 K mol^{-1}, which increases to *ca.* 244 cm^3 K mol^{-1} when the temperature is lowered to 15 K (at a field of 1000 Oe, Fig. 3d). The compound contains altogether 18 Mn^{III} S = 2 and three S = 5/2 Mn^{II} metal ions, that gives rise to a Curie constant of 67.125 cm^3 K mol^{-1} that compares well with the Curie constant (C = 66 cm^3 K mol^{-1}) obtained from the Curie–Weiss fit of the data above 100 K. The presence of ferromagnetic couplings is confirmed by the positive Weiss constant (θ = +46 K) and the increase of the χT product. These ferromagnetic interactions are necessary localized within the $\mathbf{Mn_{15}P_{10} \subset Cl_4}$ complex core as the $[Cl \subset Mn_6(\textit{tert}\text{-butyl-}PO_3)_8]^+$ counterion is known to display antiferromagnetic interactions and thus possess a diamagnetic ground state (Fig. 3c).[13c] Thus, considering the low temperature χT product of 244 cm^3 K mol^{-1} and the high field magnetization at 1.85 K (that reaches relatively fast 45μ_B at 2 T and then slowly 55.4μ_B at 7 T), this pentadeca-

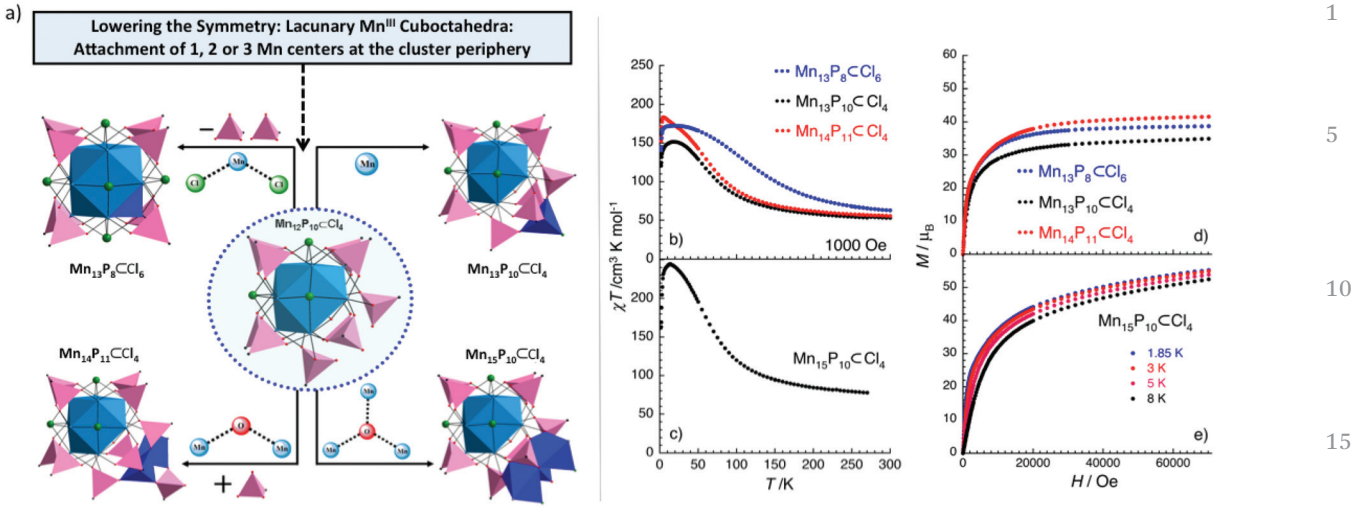

Fig. 3 (a) Representation of the structural evolution from the intermediate cluster $Mn_{12}P_{10} \subset Cl_4$ towards $Mn_{13}P_8 \subset Cl_6$, $Mn_{13}P_{10} \subset Cl_4$, $Mn_{14}P_{11} \subset Cl_4$ and $Mn_{15}P_{10} \subset Cl_4$. The blue polyhedra highlight the attachment of the additional Mn atoms to $Mn_{12}P_{10} \subset Cl_4$. (b)–(e) Magnetic properties of $Mn_{13}P_8 \subset Cl_6$, $Mn_{13}P_{10} \subset Cl_4$, $Mn_{14}P_{11} \subset Cl_4$ and $Mn_{15}P_{10} \subset Cl_4$: temperature dependence of the χT product in a 1000 Oe dc field for (b) $Mn_{13}P_8 \subset Cl_6$, $Mn_{13}P_{10} \subset Cl_4$, $Mn_{14}P_{11} \subset Cl_4$ and (c) $Mn_{15}P_{10} \subset Cl_4$. Field dependence of magnetisation for (d) $Mn_{13}P_8 \subset Cl_6$, $Mn_{13}P_{10} \subset Cl_4$ and $Mn_{14}P_{11} \subset Cl_4$ at 1.85 K and (e) $Mn_{15}P_{10} \subset Cl_4$ at the temperatures indicated with scanning at 80–400 Oe min^{-1} for $H < 1$ T and 500–2500 Oe min^{-1} for $H > 1$ T.

Table 3 Constitutional relationship between cluster composition/topology and structure-influencing chloride concentration during the preparation of the compounds

Molar ratio of choride : phosphonate (Cl : P) used for the synthesis of the coordination clusters	6 : 1	4 : 1		3 : 1	2 : 1
Building units	$\{Mn_{13}P_8\}$	$\{Mn_{12}P_8\} + \{MnP_2\}$	$\{Mn_{12}P_8\} + \{Mn_3P_2\}$	$\{Mn_{12}P_8\} + \{P_2\}$ $\{Mn_{12}P_8\} + \{Mn_3P_2\}$ $\{Mn_{12}P_8\} + \{MnP_2\}$	$\{Mn_{12}P_8\} + \{Mn_2P_3\}$
Structure-stabilising chloride ions	$\{Cl_6\}$	$\{Cl_4\}$	$\{Cl_4\}$	$\{Cl_4\}$	$\{Cl_4\}$
Number of square $\{Mn_4\}$ sub-units in the final species	6	4	4	4	4
Crystallizing coordination cluster	$\mathbf{Mn_{13}P_8 \subset Cl_6}$	$\mathbf{Mn_{13}P_{10} \subset Cl_4}$	$\mathbf{Mn_{15}P_{10} \subset Cl_4}$	$\mathbf{Mn_{12}P_{10} \subset Cl_4}$ $\mathbf{Mn_{13}P_{10} \subset Cl_4}$ $\mathbf{Mn_{15}P_{10} \subset Cl_4}$	$\mathbf{Mn_{14}P_{11} \subset Cl_4}$

nuclear $\mathbf{Mn_{15}P_{10} \subset Cl_4}$ complex should have a spin ground state of about 45/2. In addition, the field-dependences of the magnetization (Fig. 3e), which almost saturate at high dc field, confirm that the core structures of these Keggin- and Lacunary-type clusters possess a weak magnetic anisotropy. This observation is in agreement with the structural features of the compounds and the concentric orientations of the Mn^{III} Jahn–Teller axes toward the central halide unit. Despite their high spin ground states, $\mathbf{Mn_{13}P_8 \subset Cl_6}$, $\mathbf{Mn_{13}P_{10} \subset Cl_4}$, $\mathbf{Mn_{14}P_{11} \subset Cl_4}$ and $\mathbf{Mn_{15}P_{10} \subset Cl_4}$ do not show any evidence of Single-Molecule Magnet properties by *ac* susceptibility measurements.

Synthetic approach to SMMs: distorted cuboctahedral Mn clusters

To exploit the here presented system in which the Mn spin centers are generally ferromagnetically coupled, for the preparation of SMMs, synthetic methodologies were required to influence the orientation of the Jahn–Teller axes to induce magnetic anisotropy. Considering the structural characteristics of the present system, we anticipated that this might be achievable through the suppression of the structure-directing influence of the Cl^- ions. When the more polar coordinative solvent methanol is used instead of acetonitrile under synthetic conditions that led to $\mathbf{Mn_{14}P_{11} \subset Cl_4}$, a new less-symmetrical but related cluster, $\mathbf{Mn_{15}P_{12} \subset Cl_2}$, can be isolated (Fig. 4a, b and Table 1). In this species, methanol molecules not only act as terminal ligands but also bridge as deprotonated μ-CH_3O^- ligands between Mn^{III} ions, significantly reducing the influence of the Cl^- ions. In the $\mathbf{Mn_{15}P_{12} \subset Cl_2}$ core, only two Cl^- ions are retained and stabilize two $\{Mn_4\}$ squares. The lack of four Cl^- ligands results in the removal of two vertexes of the original $\{Mn_{12}\}$ cuboctahedron. Here the central Mn^{II} ion is now connected to 10 surrounding Mn^{III} metal ions to form a bi-lacunary-type structure whereby the observed $\mathbf{Mn_{15}P_{12} \subset Cl_2}$ structure results from the attachment of a

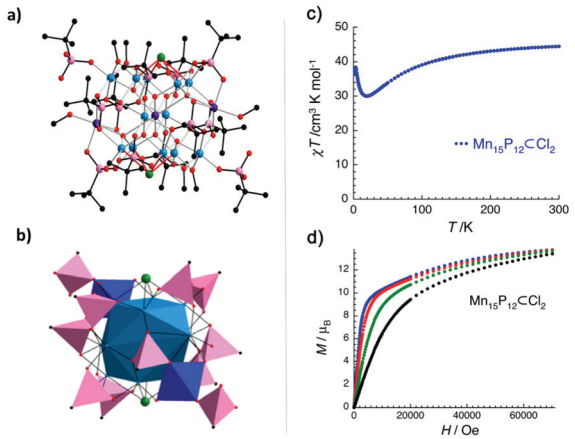

Fig. 4 (a) and (b) Structure and polyhedral representation of $\mathbf{Mn_{15}P_{12} \subset Cl_2}$. Color code: Mn^{III} violet, Mn^{III} light blue, Mn^{IV} Kelly green, P pink, O red, C black. (c) Dependence of the χT product in a 1000 Oe dc field for $\mathbf{Mn_{15}P_{12} \subset Cl_2}$. (d) Field dependence of magnetisation for $\mathbf{Mn_{15}P_{12} \subset Cl_2}$ at the temperatures indicated with scanning at 80–400 Oe min^{-1} for $H < 1$ T and 500–2500 Oe min^{-1} for $H > 1$ T.

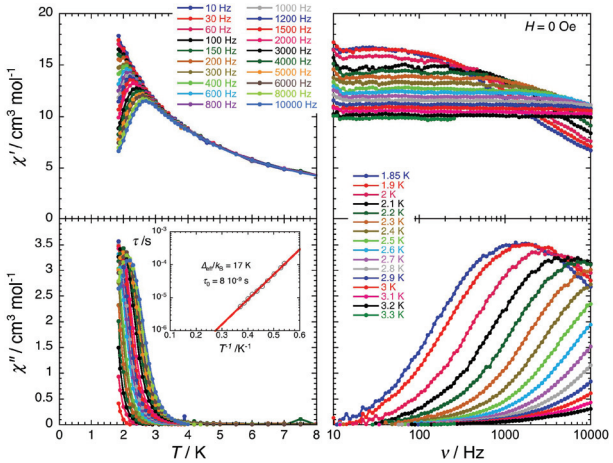

Fig. 5 Temperature (left) and frequency (right) dependences of the real (χ', top) and imaginary (χ'', bottom) components of the ac susceptibility, between 1.8 and 6 K and between 10 and 10 000 Hz respectively, for $\mathbf{Mn_{15}P_{12} \subset Cl_2}$ without dc field. Solid lines are visual guides. Inset: Temperature dependence of the relaxation time, τ, plotted as τ *versus* T^{-1}. The data points are obtained from the generalized Debye fitting of the frequency dependence of the imaginary component of the ac susceptibility shown in the main figure. The solid line is the best fits to the Arrhenius law discussed in the text.

$\{Mn^{II}Mn^{III}\}$ unit at each lacunary face. Whilst the central Mn positions in $\mathbf{Mn_{15}P_{12} \subset Cl_2}$ closely relate to those in the archetype $\mathbf{Mn_{13}P_8 \subset Cl_6}$ complex and its described family, the orientations of the Jahn–Teller axes (as determined by the Cl^- positions) differ significantly to give a more anisotropic vectorial distribution.

SMM properties of $\mathbf{Mn_{15}P_{12} \subset Cl_2}$

The magnetic properties of $\mathbf{Mn_{15}P_{12} \subset Cl_2}$ were studied on powdered microcrystalline samples. As shown in Fig. 4c, the room temperature χT product is 44.6 cm^3 K mol^{-1} in good agreement with the presence of twelve $S = 2$ Mn^{III} and three $S = 5/2$ Mn^{II} magnetic center ($C = 49.125$ cm^3 K mol^{-1}). The slightly low value of the χT product is likely the result of dominating antiferromagnetic interactions within the $\mathbf{Mn_{15}P_{12} \subset Cl_2}$ complex, which are clearly seen by the χT decrease observed when the temperature is lowered (to 29.1 cm^3 K mol^{-1} at 20 K). This is confirmed by the Curie–Weiss fit of the experimental data that confirms the presence of antiferromagnetic interactions with a Weiss constant of −21(1) K and gives a Curie constant of 47.9 cm^3 K mol^{-1} closer to the expected one. Below 20 K, the χT product at 1000 Oe for $\mathbf{Mn_{15}P_{12} \subset Cl_2}$ increases to 38.3 cm^3 K mol^{-1} at 3 K despite the presence of dominant antiferromagnetic interactions between the Mn spin centers. This thermal behavior suggests the presence of a relatively large spin ground state estimated around $S_T = 17/2$. The field-dependence of the magnetization for $\mathbf{Mn_{15}P_{12} \subset Cl_2}$ has been also measured at temperatures below 8 K (Fig. 4d). The magnetization at low field experiences a rapid increase without inflexion point confirming the presence of a non-zero spin-ground state for this complex. The high field behaviour that displays a non-linear increase without clear saturation even at 1.8 K at 7 T, can be attributed to a significantly magnetic anisotropy of the $\mathbf{Mn_{15}P_{12} \subset Cl_2}$ core. At 1.8 K and 7 T, the magnetization reaches 13.8μ_B which confirms a relatively large spin ground state for $\mathbf{Mn_{15}P_{12} \subset Cl_2}$.

Motivated by the presence of a significant magnetic anisotropy and a large spin ground state in $\mathbf{Mn_{15}P_{12} \subset Cl_2}$, the magnetization dynamics were investigated by ac susceptibility measuremets in zero dc field above 1.8 K (for frequencies around 10000 Hz, Fig. 5). These measurements reveal the presence of slow relaxation of the magnetization as indicated by the appearance of a frequency dependent out-of-phase ac signal below 4 K. Therefore temperature and frequency dependences of the zero-field ac susceptibility have been measured and the temperature dependence of the relaxation time, τ, have been deduced from the maximum of the χ' *vs.* ν data. In accordance to the Arrhenius law, the exponential increase of the relaxation with decreasing temperature (see inset of Fig. 5) allowed us to determine the energy gap of the thermally activated regime at 17 K with τ_0 of *ca.* 8.0×10^{-9} s for $\mathbf{Mn_{15}P_{12} \subset Cl_2}$. It is worth noting that the ac susceptibility measurements with application of small dc fields reveal weak influences of the quantum relaxation pathway above 1.8 K. These studies of the magnetic properties render $\mathbf{Mn_{15}P_{12} \subset Cl_2}$ undoubtedly as SMMs.

Symmetry and magnetic properties

The described structures and associated magnetic properties highlight a concept for the synthesis of SMMs upon imposing structural anisotropy on isotropic high-spin complexes. Fig. 6 visualizes the structure-influencing effect of halide ions on organophosphonate-stabilised complexes with cuboctahedral Mn topology. It is well established that the magnetic anisotropy of Mn^{III}-based coordination clusters correlate to the vectorial summation of the single-ion anisotropy of the Mn

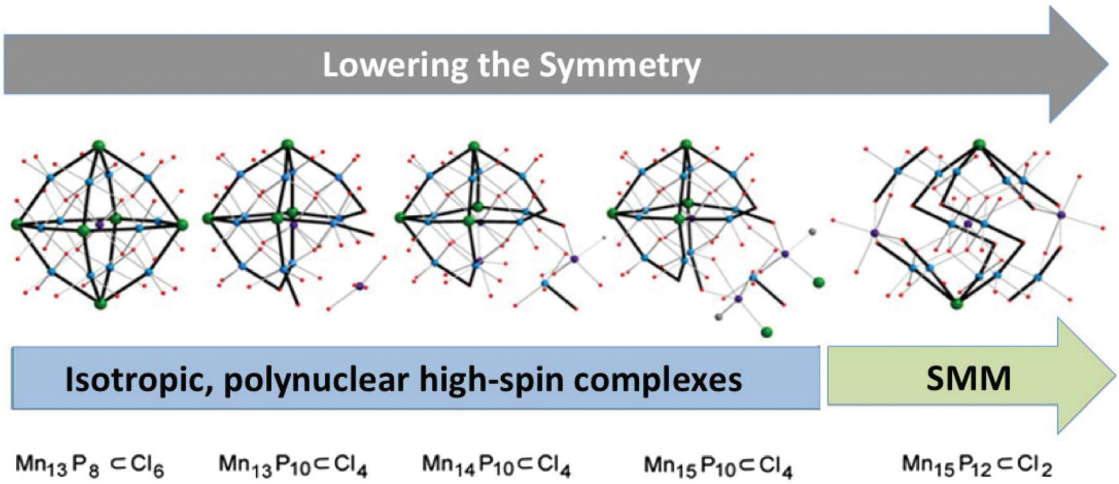

Fig. 6 Structure-influencing effect of halide ions on organophosphonate-stabilised clusters with cuboctahedral Mn topology, highlighting the construction of SMMs upon imposing structural anisotropy on isotropic high-spin clusters. Jahn–Teller elongated axes of Mn^{III} are highlighted in bold.

centers, which are distinctively determined by the relative orientations of their Jahn–Teller axes. Considering the positions of the Cl^- ions that reside in Jahn–Teller sites and locate in the three orthogonal 90° directions, the magnetic anisotropy arising from the cuboctahedral cores in $\mathbf{Mn_{13}P_8 \subset Cl}$, $\mathbf{Mn_{13}P_{10} \subset Cl_4}$, $\mathbf{Mn_{14}P_{11} \subset Cl_4}$ and $\mathbf{Mn_{15}P_{10} \subset Cl_4}$ is expected to be negligible. In agreement with this model, these species do not show SMM properties, despite stabilizing high-spin ground states. In the less-symmetrical complex, $\mathbf{Mn_{15}P_{12} \subset Cl_2}$, the reduced halide content or the relative locations of the halide ions result in a re-orientation of the individual Jahn–Teller axes to give Ising-type magnetic species. In contrast to the isotropic high-spin complexes, the latter compound is a SMM.

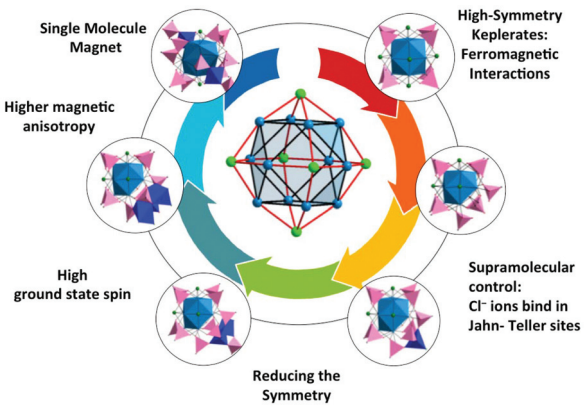

Fig. 7 Pictographical representation which summarizes the key characteristics investigated Mn reaction system and highlights the structure-influencing effect of halide ions.

Conclusions

The here presented methodology in which halide ions are utilized to influence the assembly and symmetry of Mn complexes allowed us to prepare a homologue series of structurally-related cores and modulate the magnetic properties of high-spin complexes to produce a SMM. The applied strategy is distinctive from purely serendipitous synthetic approaches to high-nuclearity SMMs, which often hamper detailed structure–property correlations due to the prevalence of wide-ranging, diverse structural topologies. The applied concept is comparable the template effect that was observed in a previously studied polyoxovanadate system, where the Cl^- ions stabilize the formation of square $\{V_4\}$ units and direct their assembly to form hollow polyoxovanadate cages or molecular capsules (Fig. S9†).[10a] In these systems, the halide ions act as weakly coordinating nucleophiles (Lewis bases) that donate electron density to square pyramidal vanadate units that condense into convex entities encapsulating the templates as guests. Tetragonally distorted Jahn–Teller Mn^{III} ions that form upon com-proportionation of Mn^{II} and Mn^{VII} species offer two preferential binding sites for weakly binding Cl^- ions in their apical positions; the prevailing non-directional Coulomb forces and the isotropic ionic nature enable halide ions to act as a bridging ligands that preferentially reside on the outside of condensed, symmetrical Mn coordination clusters. The here reported key characteristics of the investigated Mn reaction system and the structure-influencing effect of halide ions are summarized in Fig. 7. Preliminary, ongoing experiments using heavy transition metal ions (*e.g.* Dy^{III} and Gd^{III}) suggest that the applied approach is also applicable in other highly ionic reaction systems that give rise to larger magnetic anisotropies and increase blocking temperatures of the resulting SMMs.

Acknowledgements

The authors thank the Science Foundation Ireland (SFI; 13/IA/1896), the European Research Council (CoG 2014-647719), the

Irish Research Council (Fellowship for L. Z.), the National Natural Science Foundation of China (NSFC 21501176), the University of Bordeaux, the Région Aquitaine, the GIS Advanced Materials in Aquitaine (COMET Project) and the CNRS for financial support. We acknowledge Dr Martin Feeney for help with the mass spectrometry analyses.

Notes and references

1 (*a*) D. Gatteschi, R. Sessoli and J. Villain, *Molecular Nanomagnets*, Oxford University Press, New York, 2007; (*b*) L. Bogani and W. Wernsdorfer, *Nat. Mater.*, 2008, **7**, 179; (*c*) M. Murugesu, M. Habrych, W. Wernsdorfer, K. A. Abboud and G. Christou, *J. Am. Chem. Soc.*, 2004, **126**, 4766; (*d*) W. G. Wang, A. J. Zhou, W. X. Zhang, M. L. Tong, X. M. Chen, M. Nakano, C. C. Beedle and D. N. Hendrickson, *J. Am. Chem. Soc.*, 2007, **129**, 1014; (*e*) Y. F. Bi, X. T. Wang, W. P. Liao, X. F. Wang, X. W. Wang, H. J. Zhang and S. Gao, *J. Am. Chem. Soc.*, 2009, **131**, 11650; (*f*) L. Lisnard, F. Tuna, A. Candini, M. Affronte, R. E. P. Winpenny and E. J. L. McInnes, *Angew. Chem., Int. Ed.*, 2008, **47**, 9695; S. Cardona-Serra, J. M. Clemente-Juan, E. Coronado, A. Gaita-Arino, A. Camon, M. Evangelisti, F. Luis, M. J. Martinez-Perez and J. Sese, *J. Am. Chem. Soc.*, 2012, **134**, 14982.

2 (*a*) X. J. Kong, L. S. Long, Z. P. Zheng, R. B. Huang and L. S. Zheng, *Acc. Chem. Res.*, 2010, **43**, 201; (*b*) Y. Z. Zheng, M. Evangelisti and R. E. P. Winpenny, *Angew. Chem., Int. Ed.*, 2011, **50**, 3692; (*c*) Y. Z. Zheng, M. Evangelisti and R. E. P. Winpenny, *Chem. Sci.*, 2011, **2**, 99; (*d*) G. Karotsis, S. Kennedy, S. J. Teat, C. M. Beavers, D. A. Fowler, J. J. Morales, M. Evangelisti, S. J. Dalgarno and E. K. Brechin, *J. Am. Chem. Soc.*, 2010, **132**, 12983; (*e*) J. B. Peng, Q. C. Zhang, X. J. Kong, Y. Z. Zheng, Y. P. Ren, L. S. Long, R. B. Huang, L. S. Zheng and Z. P. Zheng, *J. Am. Chem. Soc.*, 2012, **134**, 3314; (*f*) Y. Z. Zheng, M. Evangelisti, F. Tuna and R. E. P. Winpenny, *J. Am. Chem. Soc.*, 2012, **134**, 1057.

3 (*a*) M. Atanasov, P. Surawatanawong, K. Wieghardt and F. Neese, *Coord. Chem. Rev.*, 2013, **257**, 27; (*b*) M. Atanasov, J. M. Zadrozny, J. R. Long and F. Neese, *Chem. Sci.*, 2013, **4**, 139; (*c*) E. Cremades, S. Gomez-Coca, D. Aravena, S. Alvarez and E. Ruiz, *J. Am. Chem. Soc.*, 2012, **134**, 10532.

4 (*a*) R. Sessoli and A. K. Powell, *Coord. Chem. Rev.*, 2009, **253**, 2328; (*b*) D. Gatteschi and R. Sessoli, *Angew. Chem., Int. Ed.*, 2003, **42**, 268; (*c*) E. K. Brechin and G. Aromi, *Struct. Bonding*, 2006, **22**, 1; (*d*) N. Domingo, E. Bellido and D. Ruiz-Molina, *Chem. Soc. Rev.*, 2012, **41**, 258; (*e*) M. Clemente-Leon, H. Soyer, E. Coronado, C. Mingotaud, C. J. Gomez-Garcia and P. Delhaes, *Angew. Chem., Int. Ed.*, 1998, **37**, 2842.

5 (*a*) R. E. P. Winpenny, *J. Chem. Soc., Dalton Trans. 1*, 2002; (*b*) R. W. Saalfrank, H. Maid and A. Scheurer, *Angew. Chem., Int. Ed.*, 2008, **47**, 8794; (*c*) G. E. Kostakis, S. P. Perlepes, V. A. Blatov, D. M. Proserpio and A. K. Powell, *Coord. Chem. Rev.*, 2012, **256**, 1246; (*d*) J. P. Sauvage, *Perspectives in Supramolecular Chemistry: Transition Metals in Supramolecular Chemistry*, John Wiley & Sons, Ltd, Chichester, UK, 1999, vol. 5.

6 (*a*) J. J. Novoa, M. Deumal and J. Jornet-Somoza, *Chem. Soc. Rev.*, 2011, **40**, 3182; (*b*) M. J. Martinez-Perez, S. Cardona-Serra, C. Schlegel, F. Moro, P. J. Alonso, H. Prima-Garcia, J. M. Clemente-Juan, M. Evangelisti, A. Gaita-Arino, J. Sese, J. van Slageren, E. Coronado and F. Luis, *Phys. Rev. Lett.*, 2012, **108**, 247213; (*c*) J. J. Novoa, D. Braga and L. Addadi, *Engineering of Crystalline Materials Properties*, Springer, Dordrecht, 2008.

7 (*a*) M. Manoli, A. Collins, S. Parsons, A. Candini, M. Evangelisti and E. K. Brechin, *J. Am. Chem. Soc.*, 2008, **130**, 11129; (*b*) M. Manoli, R. D. L. Johnstone, S. Parsons, M. Murrie, M. Affronte, M. Evangelisti and E. K. Brechin, *Angew. Chem., Int. Ed.*, 2007, **46**, 4456; (*c*) M. Soler, W. Wernsdorfer, K. Folting, M. Pink and G. Christou, *J. Am. Chem. Soc.*, 2004, **126**, 2156; (*d*) R. T. W. Scott, S. Parsons, M. Murugesu, W. Wernsdorfer, G. Christou and E. K. Brechin, *Angew. Chem., Int. Ed.*, 2005, **44**, 6540; (*e*) S. Maheswaran, G. Chastanet, S. J. Teat, T. Mallah, R. Sessoli, W. Wernsdorfer and R. E. P. Winpenny, *Angew. Chem., Int. Ed.*, 2005, **44**, 5044; (*f*) A. M. Ako, I. J. Hewitt, V. Mereacre, R. Clérac, W. Wernsdorfer, C. E. Anson and A. K. Powell, *Angew. Chem., Int. Ed.*, 2006, **45**, 4926; (*g*) E. K. Brechin, R. A. Coxall, A. Parkin, S. Parsons, P. A. Tasker and R. E. P. Winpenny, *Angew. Chem., Int. Ed.*, 2001, **40**, 2700.

8 (*a*) H. Miyasaka, K. Nakata, L. Lecren, C. Coulon, Y. Nakazawa, T. Fujisaki, K. Sugiura, M. Yamashita and R. Clérac, *J. Am. Chem. Soc.*, 2006, **128**, 3770; (*b*) E. E. Moushi, T. C. Stamatatos, W. Wernsdorfer, V. Nastopoulos, G. Christou and A. J. Tasiopoulos, *Angew. Chem., Int. Ed.*, 2006, **45**, 7722; (*c*) E. E. Moushi, C. Lampropoulos, W. Wernsdorfer, V. Nastopoulos, G. Christou and A. J. Tasiopoulos, *J. Am. Chem. Soc.*, 2010, **132**, 16146; (*d*) T. C. Stamatatos, K. A. Abboud, W. Wernsdorfer and G. Christou, *Angew. Chem., Int. Ed.*, 2007, **46**, 884; (*e*) M. D. Godbole, O. Roubeau, R. Clérac, H. Kooijman, A. L. Spek and E. Bouwman, *Chem. Commun.*, 2005, 3715; (*f*) C. M. Liu, R. G. Xiong, D. Q. Zhang and D. B. Zhu, *J. Am. Chem. Soc.*, 2010, **132**, 4044; (*g*) T. O. Chimamkpam, R. Clérac, D. Mitcov, B. Twamley, M. Venkatesan and W. Schmitt, *Dalton Trans.*, 2016, **45**, 1349; (*h*) G. N. Newton, S. Yamashita, K. Hasumi, J. Matsuno, N. Yoshida, M. Nihei, T. Shiga, M. Nakano, H. Nojiri, W. Wernsdorfer and H. Oshio, *Angew. Chem., Int. Ed.*, 2011, **50**, 5715.

9 (*a*) M. Nakano and H. Oshio, *Chem. Soc. Rev.*, 2011, **40**, 3239; (*b*) V. M. Mereacre, A. M. Ako, R. Clérac, W. Wernsdorfer, G. Filoti, J. Bartolome, C. E. Anson and A. K. Powell, *J. Am. Chem. Soc.*, 2007, **129**, 9248; (*c*) H. Oshio and M. Nakano, *Chem. – Eur. J.*, 2005, **11**, 5178; (*d*) Y. Z. Zheng, W. Xue, W. X. Zhang, M. L. Tong and X. M. Chen, *Inorg. Chem.*, 2007, **46**, 6437; (*e*) H. Miyasaka, A. Saitoh and S. Abe, *Coord. Chem. Rev.*, 2007, **251**,

2622; (*f*) P. Parois, S. A. Moggach, J. Sanchez-Benitez, K. V. Kamenev, A. R. Lennie, J. E. Warren, E. K. Brechin, S. Parsons and M. Murrie, *Chem. Commun.*, 2010, **46**, 1881.

10 (*a*) L. Zhang and W. Schmitt, *J. Am. Chem. Soc.*, 2011, **133**, 11240; (*b*) S. Leininger, J. Fan, M. Schmitz and P. Stang, *J. Proc. Nat. Acad. Sci. U. S. A.*, 2000, **97**, 1380; (*c*) H. N. Miras, G. J. T. Cooper, D. L. Long, H. Bogge, A. Muller, C. Streb and L. Cronin, *Science*, 2010, **327**, 72; (*d*) A. Müller, K. Hovemeier and R. Rohlfing, *Angew. Chem., Int. Ed.*, 1992, **31**, 1192; (*e*) Y. P. Xie and T. C. W. Mak, *J. Am. Chem. Soc.*, 2011, **133**, 3760.

11 (*a*) R. G. Finke, M. W. Droege, J. C. Cook and K. S. Suslick, *J. Am. Chem. Soc.*, 1984, **106**, 5750; (*b*) C. S. Truebenbach, M. Houalla and D. M. Hercules, *J. Mass Spectrom.*, 2000, **35**, 1121; (*c*) M. Bonchio, O. Bortolini, V. Conte and A. Sartorel, *Eur. J. Inorg. Chem.*, 2003, 699; (*d*) R. Llusar, I. Sorribes and C. Vicent, *J. Cluster Sci.*, 2009, **20**, 177; (*e*) C. I. Onet, L. Zhang, R. Clérac, J. B. Jean-Denis, M. Feeney, T. McCabe and W. Schmitt, *Inorg. Chem.*, 2011, **50**, 604.

12 (*a*) H. N. Miras, E. F. Wilson and L. Cronin, *Chem. Commun.*, 2009, 1297; (*b*) R. Tsunashima, D. L. Long, H. N. Miras, D. Gabb, C. P. Pradeep and L. Cronin, *Angew. Chem., Int. Ed.*, 2010, **49**, 113; (*c*) E. F. Wilson, H. Abbas, B. J. Duncombe, C. Streb, D. L. Long and L. Cronin, *J. Am. Chem. Soc.*, 2008, **130**, 13876; (*d*) Y. F. Song, D. L. Long, S. E. Kelly and L. Cronin, *Inorg. Chem.*, 2008, **47**, 9137; (*e*) J. Yan, D. L. Long, E. F. Wilson and L. Cronin, *Angew. Chem., Int. Ed.*, 2009, **48**, 4376.

13 (*a*) L. Zhang, R. Clérac, P. Heijboer and W. Schmitt, *Angew. Chem., Int. Ed.*, 2012, **51**, 3007; (*b*) L. Zhang, R. Clérac, C. I. Onet, M. Venkatesan, P. Heijboer and W. Schmitt, *Chem. – Eur. J.*, 2012, **18**, 13984; (*c*) L. Zhang, B. Marzec, R. Clérac, Y. H. Chen, H. Z. Zhang and W. Schmitt, *Chem. Commun.*, 2013, **49**, 66; (*d*) L. Zhang, C. I. Onet, R. Clérac, M. Rouzieres, B. Marzec, M. Boese, M. Venkatesan and W. Schmitt, *Chem. Commun.*, 2013, **49**, 7400.

14 (*a*) E. V. Chubarova, M. H. Dickman, B. Keita, L. Nadjo, F. Miserque, M. Mifsud, I. W. C. E. Arends and U. Kortz, *Angew. Chem., Int. Ed.*, 2008, **47**, 9542; (*b*) N. V. Izarova, M. H. Dickman, R. N. Biboum, B. Keita, L. Nadjo, V. Ramachandran, N. S. Dalal and U. Kortz, *Inorg. Chem.*, 2009, **48**, 7504; (*c*) M. Barsukova, N. V. Izarova, R. N. Biboum, B. Keita, L. Nadjo, V. Ramachandran, N. S. Dalal, N. S. Antonova, J. J. Carbo, J. M. Poblet and U. Kortz, *Chem. – Eur. J.*, 2010, **16**, 9076; (*d*) M. Barsukova-Stuckart, N. V. Izarova, R. Barrett, Z. X. Wang, J. van Tol, H. W. Kroto, N. S. Dalal, B. Keita, D. Heller and U. Kortz, *Chem. – Eur. J.*, 2012, **18**, 6167; (*e*) M. Barsukova-Stuckart, N. V. Izarova, R. A. Barrett, Z. X. Wang, J. van Tol, H. W. Kroto, N. S. Dalal, P. Jimenez-Lozano, J. J. Carbo, J. M. Poblet, M. S. von Gernler, T. Drewello, P. de Oliveira, B. Keita and U. Kortz, *Inorg. Chem.*, 2012, **51**, 13214.

15 (*a*) L. F. Jones, E. K. Brechin, D. Collison, J. Raftery and S. J. Teat, *Inorg. Chem.*, 2003, **42**, 6971; (*b*) S. L. Benjamin, W. Levason and G. Reid, *Chem. Soc. Rev.*, 2013, **42**, 1460.